Canadian Conference - Pacific Conference on Earthquake Engineering 2023

Vancouver, British Columbia

June 25th – June 30th, 2023

Seismic Design and Analysis of Bridge Piers Reinforced with Rebar Types of CSA 500W, CSA 400W, and ASTM 1035 Grade 690

Sisay Tadele[1], Han Li[2], Qi Zhang[3], Faroque Hossain[4], M. Shahria Alam[5*], Alireza Ahmadnia[6], Jianping Jiang[7]

[1]MASc Student, School of Engineering, The University of British Columbia, Canada
[2]Postdoctoral Fellow, School of Engineering, The University of British Columbia, Canada
[3]Postdoctoral Fellow, School of Engineering, The University of British Columbia, Canada, Instructor, British Columbia Institute of Technology
[4]PhD Candidate, School of Engineering, The University of British Columbia, Canada
[5]Professor & Tier-1 Principal's Research Chair, School of Engineering, The University of British Columbia, Canada
[6]Chief Bridge Engineer, BC Ministry of Transportation and Infrastructure, Canada
[7]National Practice Leader, Bridges & Civil Structures, WSP Canada, Canada
[*]shahria.alam@ubc.ca (Corresponding Author)

ABSTRACT

The use of high-strength steel (HSS) reinforcement in concrete structures has been gaining popularity. However, concerns have been raised about the ductility of structures reinforced with HSS, particularly when subjected to strong earthquakes. To this end, this research compares the seismic performance of bridge piers constructed with three different types of rebars, namely regular rebar CSA 400W, and HSS rebars of CSA 500-C, and ASTM 1035 Grade 690. The reinforced concrete (RC) pier design matrix comprising several models with varying design parameters was generated. Nonlinear static pushover analyses were then conducted on each pier model to compare their drift ratios at various damage states. To further compare the seismic performance of these bridge piers, dynamic nonlinear time history analyses were conducted, and their seismic performances were presented through fragility curves for the various damage states. This study aims to provide engineers with useful information regarding the comparative seismic response of piers reinforced with regular and HSS reinforcement, as well as the seismic design of RC bridge piers using HSS rebars.

Keywords: High strength steel rebar, bridge pier, drift ratio, damage states, fragility curve.

INTRODUCTION

Bridges are essential components of transportation infrastructure, connecting cities and regions. Damage to bridge structures can cause severe disruptions to traffic, resulting in economic losses and even fatalities. To improve the seismic performance of bridges, engineers have implemented several measures, such as using stronger materials including high-strength concrete and steel. However, before using high-strength steel (HSS) reinforcement in reinforced concrete (RC) bridge piers located in seismic zones, it is important to address some critical issues. Firstly, it is crucial to ensure that the increased strength does not compromise the ductility of the structures. Secondly, it is essential to be able to model the post-yielding behaviour of RC members with HSS reinforcement. Bridge piers are ductile members, and members connected to piers, such as pier caps and foundations, are capacity-protected members. Before the implementation of HSS reinforcement, engineers have to be able to predict the overstrength/probable resistance of bridge piers so that other capacity-protected members can be properly designed.

This study performs a preliminary evaluation and comparison of RC piers with different types of reinforcing steel. The comparison of seismic performance is achieved through fragility analysis, which has been widely employed to evaluate probability of reaching a given damage state for given levels of seismic intensities, such as Peak Ground Acceleration (PGA) [1-2]. For instance, Karim et. al [3] designed bridge piers in accordance with Japanese seismic design guidelines and developed their corresponding fragility curves. Nonlinear dynamic response evaluations were carried out using strong motion records from Japan and the US, and the damage indices for the bridge piers were determined. Based on a collection of ground motions observed in Korea, Nguyen et al. [4] also developed seismic fragility curves for bridge piers. A number of damage states were identified by nonlinear time history studies using a damage index expressed in terms of the column displacement ductility ratio. Avşar et al. [5] developed analytical fragility curves for bridges built in Turkey before 1990. The seismic response of the bridges was analyzed by conducting a component-based approach where several engineering demand parameters were employed to study seismic response of bridge components. The study shows bridges having larger skew angles or single-column bents were the most seismically vulnerable structures. Nielson et al. [6] developed analytical fragility curves for different bridge classes common to the central and southeastern United States. The study concluded that multispan steel girder bridges are the most seismically vulnerable while single-span bridges are the least vulnerable. Billah and Alam [7] performed seismic fragility assessment of a typical multi-span highway bridge in BC considering soil-structure interaction. They concluded that although the soil–structure interaction has some effect on the component fragility, this effect is not very significant at the bridge system level. A number of studies using fragility curves can be referred to literature [8-10].

This paper compares the seismic performance of bridge piers reinforced with various types of longitudinal reinforcing steel rebars, including regular rebar CSA 400W, and HSS rebars of CSA 500-C and ASTM 1035 Grade 690. Static pushover and analytical fragility curves are presented. A number of bridge pier design were conducted considering different parameters including specified concrete strength ($\boldsymbol{f'_c}$), aspect ratio (L/D), transverse reinforcement ratio ($\boldsymbol{\rho_s}$), and axial load ratio ($\mathbf{P/A_g{\bullet}\boldsymbol{f_c}}$). However, the focus of this paper is on the effects of different types of reinforcing steel. This study aims to develop an understanding of the seismic performance of bridge piers reinforced with longitudinal rebar types of CSA 400W, CSA 500W and ASTM A1035 Grade 690 under different design scenarios.

DESIGN OF THE BRIDGE PIER

This study focuses on the seismic performance of the bridge pier models reinforced with different rebar types including CSA 400W, CSA 500W, and ASTM A1035 Grade 690. A prototype pier is first designed with CSA-400W reinforcing steel. Based on the prototype pier, a number of other equivalent designs are determined. In developing different design options, the flexural capacity of the different options remains the same as the prototype pier. To consider the potential interactions with other design parameters, other varying parameters include concrete strength, aspect ratio of the pier and transverse reinforcement ratios. Fragility curves are derived to compare the seismic performances. Numerical analyses are performed using a finite element software SeismoStruct [11].

The parameters analyzed in this paper are presented in Table 1, including aspect ratios, reinforcing steel strengths, concrete strengths, and reinforcement ratios. When re-designing the bridge piers and to achieve the same flexural capacity as the prototype bridge pier, a number of moment curvature analysis was performed in CUMBIA software [12] until the moment curvature of the prototype bridge pier and other equivalent designs are closely matched. The pier design options are developed with specified concrete strengths of 30 MPa and 45 MPa. Longitudinal reinforcement have yield strength, f_y of 440 MPa, 587.7 MPa, and 774 MPa. Two cross sections with diameters of 406 mm, and 450 mm are considered. The column sections are relatively small as some of the design options will be tested in the lab in future studies. The effect of transverse reinforcement ratio is also studied by using two types of 10M, and 20M spiral reinforcements of the same grade.

In Table 1, bridge piers are grouped into 4 categories represented by letters a, b, c and d. Within each categories, the only difference among the piers is the rebar type. For instance, 406-30-CSA-400W-a stands for bridge pier with 406 mm diameter, 30 MPa concrete strength, having longitudinal reinforcement of rebar type CSA-400W, and belongs to pier category a. The seismic performance evaluation will be focused on comparing bridge piers with different rebar types that belong to the same category, which means that the focus is on the effect of different rebar types. In Table 1, the model 406-30-CSA-400W-a is the prototype pier. All other piers are designed to have equivalent flexural strength compared with the prototype pier.

Table 1. Pier geometry and material matrix.

Specimen no.	***D* (mm)**	***f_y* (MPa)**	***f'_c* (MPa)**	**$P/Ag.f_c$ (%)**	**ρ_l (%)**	**ρ_s (%)**
406-30-CSA-400W-a	406	440.00	30.00	7.72	2.16	1.18
406-30-CSA-500W-a	406	587.70	30.00	7.72	1.70	1.18
406-30-ASTM-A1035-a	406	774.00	30.00	7.72	1.24	1.18
406-45-CSA-400W-b	406	440.00	45.00	5.15	2.01	1.18
406-45-CSA-500W-b	406	587.70	45.00	5.15	1.70	1.18
406-45-ASTM-A1035-b	406	774.00	45.00	5.15	1.08	1.18
406-30-CSA-400W	406	440.00	30.00	7.72	2.32	0.71
406-30-CSA-500W	406	587.70	30.00	7.72	1.85	0.71
406-30-ASTM-A1035-c	406	774.00	30.00	7.72	1.24	0.71
406-30-CSA-400W-d	450	440.00	30.00	6.29	1.38	1.05
406-30-CSA-500W-d	450	587.70	30.00	6.29	1.13	1.05
406-30-ASTM-A1035-d	450	774.00	30.00	6.29	0.75	1.05

Note: ***D*** is the pier diameter, f_y is the steel strength, f'_c is the concrete compressive strength, **$P/Ag.f_c$** is the axial load ratio, ρ_l is the longitudinal reinforcement ratio, ρ_s is the transverse reinforcement ratio.

NUMERICAL MODELING OF THE BRIDGE PIERS AND VALIDATION

In order to study the seismic performance of the bridge piers listed in Table 1, finite element models were created in SeismoStruct [11]. The models employed the Menegotto-Pinto steel model [13] and the Mander concrete model [14] to simulate the nonlinear material properties of the reinforcing steel rebar and concrete, respectively. The bridge piers were modeled using inelastic displacement-based elements (DBE) and were discretized into five equal-length elements along the height.

The model validation is conducted by comparing experimental results of bridge pier responses and simulated pier responses via SeismoStruct [11]. The model validations are performed for both regular steel reinforced piers and high-strength steel reinforced piers based on experimental works conducted by Moyer and Kowalsky [15] and Restrepo et al. [16], respectively as shown in Figure 1. It can be seen that the models can capture the responses of the tested columns with acceptable accuracy.

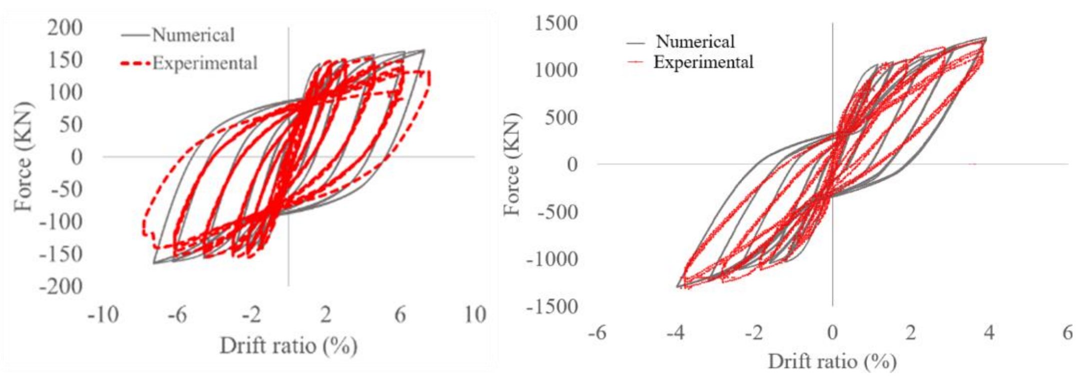

(a) *(b)*

Figure 1. SeismoStruct model verification based on: (a) Moyer and Kowalsky (2003) (b) Restrepo et al. (2006).

PUSHOVER ANALYSIS OF PIERS WITH VARIOUS REINFORCING STEEL TYPES

To perform a preliminary comparison of the effects different reinforcing steel on the lateral response of bridge piers, static pushover analysis is performed to predict the failure mechanisms and other important parameters such as base shear, yield displacement, and ductility capacity of the piers. Pushover analyses are conducted under constant gravity load of 300 kN and monotonically increasing lateral loads. During the analysis, materials strains are recorded to identify damage states as per

CHBDC [17] as shown in Table 2. The drift limit state values corresponding to the four damage states are also derived and presented in Table 2, which includes minimal damage, moderate damage, extensive damage, and probable replacement. These drifts values are established using the concrete and longitudinal reinforcement strain limits provided in Table 2.

The ratio of the drifts at Replacement to Minimal Damage range from 2.6 to 3.7, indicating the piers are generally ductile. The ratio of the drifts at Replacement to Minimal Damage can be defined as ductility. When comparing the ductility of RC piers reinforced with different reinforcing steel types, the piers with CSA 400W have an average ductility of 3.2, the piers with CSA 500W have an average ductility of 3.0. The average ductility of piers reinforced with A1035 Garde 690 is 3.4. When comparing bridge piers of the same category, i.e., within category a, b, c, or d, piers with higher strength steel reach the damage states at a higher drift ratio, meaning that high strength steel delays the damage. For instance, for bridge category a, the drift ratios corresponding to Minimal Damage are 1.94%, 1.70%, and 1.55% for piers reinforced with ASTM A1035 Garde 690 (with yield strength f_y of 774 MPa), CSA 500W (with yield strength f_y of 587.7 MPa) and CSA 400W (with yield strength f_y of 440 MPa), respectively.

Pushover curves of all piers are presented in Figure 3. The pushover curves for piers in the same category are plotted in the same figure for comparison. Although efforts have been made to design all piers with the same strength, piers with longitudinal reinforcement of ASTM A1035 Grade 690 have lower yielding base shear compared with other piers. Piers with longitudinal reinforcement of CSA 500W tend to show higher strength compared to CSA 400W.

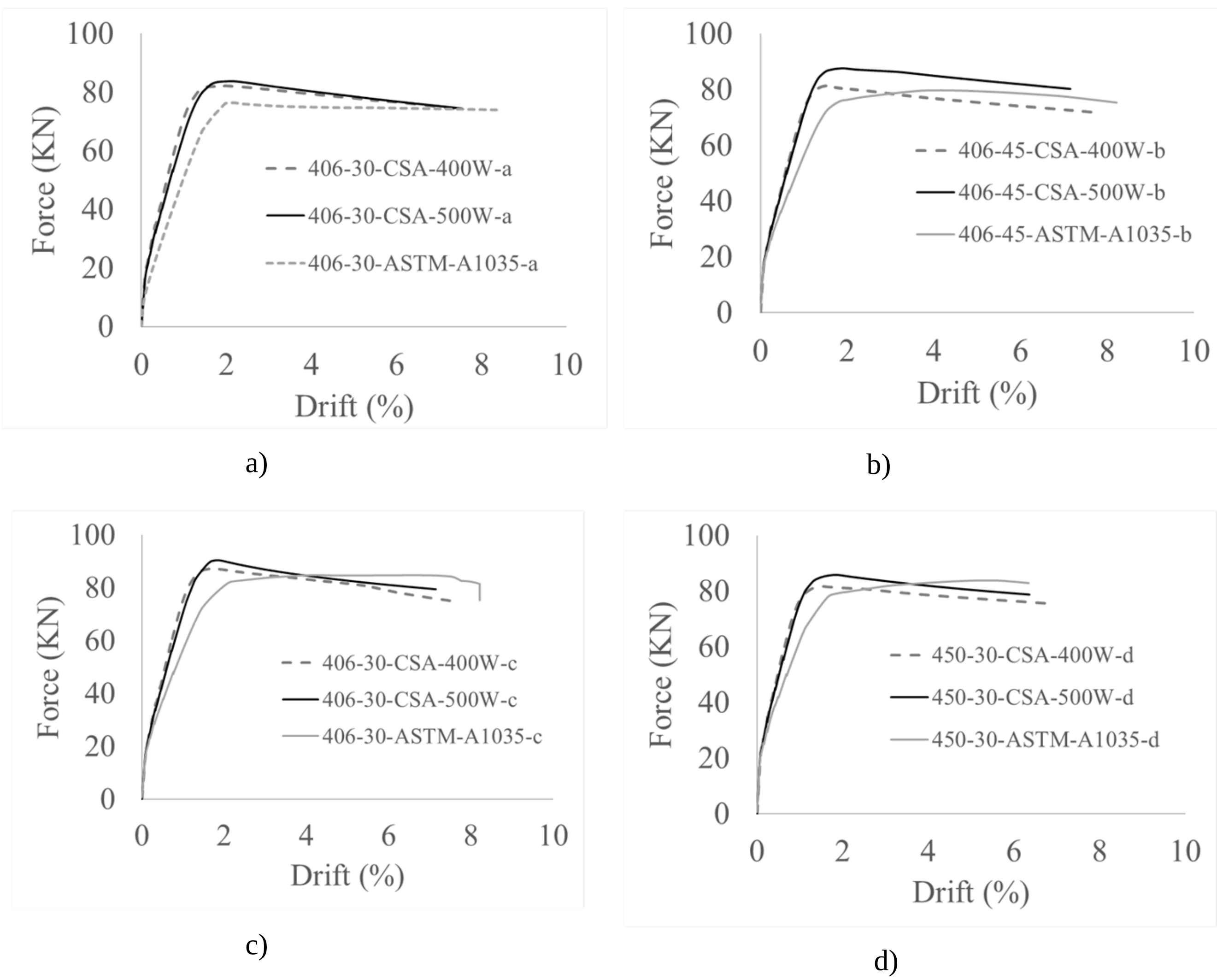

Figure 2. Pushover response curves for piers of category: a) a b) b c) c, and d) d.

Table 2. Performance limit criteria from CHBDC CSA [17]).

Service	Damage state	Material strain limits
Immediate	Minimal damage	$\varepsilon_c \leq 0.006$
		$\varepsilon_s \leq 0.01$
Limited	Repairable damage	$\varepsilon_s \leq 0.025$
service disruption	Extensive damage	$\varepsilon_s \leq 0.05$
		$\varepsilon_{cc} \leq 0.8\ \varepsilon_{cu}$
life safety	Probable replacement	$\varepsilon_s \leq 0.075$
		$\varepsilon_{cc} \leq \varepsilon_{cu}$

ε_c = concrete compressive strain; ε_s = flexural reinforcing steel strain; ε_{cc} = confined concrete strain; and ε_{cu} = ultimate confined concrete strain.

NONLINEAR TIME HISTORY AND FRAGILITY ANALYSIS OF THE BRIDGE PIERS WITH VARIOUS REINFORCEMENT TYPES

When using fragility analysis to compare the seismic performance, nonlinear time history analyses have to be performed first. For the nonlinear time history analysis, representative near-fault ground motions are selected from Pacific Earthquake Engineering Research (PEER) database [18]. The selected ground motions have a PGA ranging from 0.67g to 0.75g. Ground motions parallel to the fault are used to conduct the nonlinear time history analysis. A total of 12 ground motions are used to meet the requirements in CHBDC [17].

Ground motions are scaled to match a uniform hazard design response spectrum of Vancouver for a 2% probability of exceedance in 50 years. A wavelets algorithm by Hancock et al. [19] available in SeismoMatch [20] is used to scale the ground motions. Figure 3 shows the individual records before and after matching to the design spectrum. The Mean spectrum from the matched records is slightly greater than the target spectrum. The scaled ground motions are then utilized as the inputs of nonlinear dynamic time history analysis of the pier models.

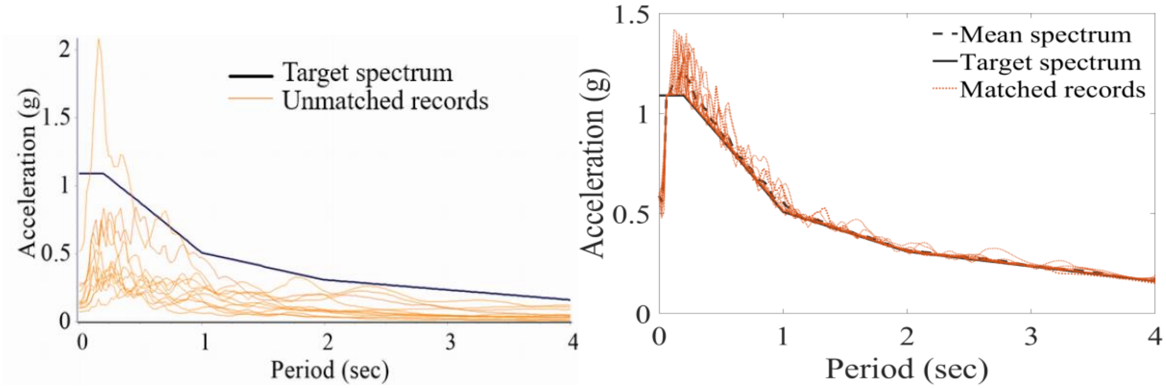

Figure 3. Ground motion records: (a) unmatched design spectrum (b) matched to design spectrum.

The seismic fragility of bridge piers was studied to compare the performance of RC piers with different types of reinforcing steel. To develop the seismic fragility curves, Incremental Dynamic Analysis (IDA) is performed, which involves conducting a series of nonlinear dynamic analyses of the structures subject to scaled ground motions.

Figure 4 presents the fragility curves for the bridge piers. The fragility curves are developed based on the results of pushover analysis and nonlinear time history analysis. Fragility curves for the bridge piers that belong to the same category are plotted in one figure for comparison. The legend of the figures is provided in the footnotes. The damage states are denoted and represented by different line colors. And line style represents different rebar types of the bridge piers, where solid line, fine dashed, and wide spaced lines denote CSA 400W, CSA 500W, and ASTM A1035 Grade 690 rebar types, respectively. The development of fragility curves is based on the procedures suggested by Cornell et al. [21].

The fragility curves show that for the same level of seismic intensity, i.e., PGA, bridge piers reinforced with ASTM A1035 Grade 690 tend to have a lower probability of failure across most PGA ranges. For instance, in the fragility curves for bridge category b (see Figure 4b below), the fragility curve for minimal damage state (colored in red) shows that piers reinforced with ASTM 1035 (i.e., wide spaced line) have a lower probability of damage compared to piers with CSA 500W, and CSA 400W. Moreover, bridge piers reinforced with CSA 500W have a lower probability of suffering minimal damage state compared to piers reinforced with CSA 400W.

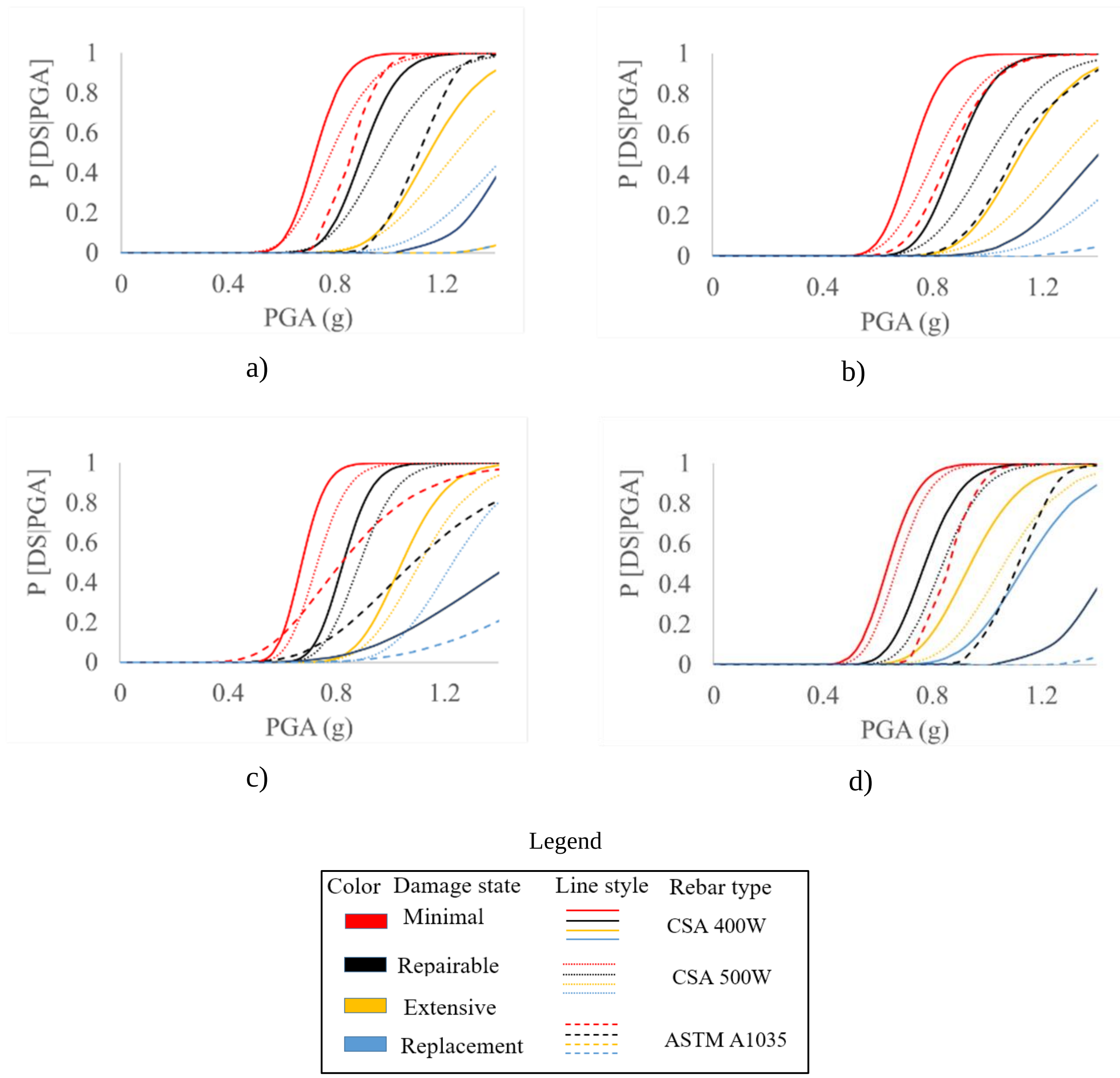

Figure 4. Fragility curve response for bridge piers of category of: a) a, b) b, c) c, and *d) d.*

CONCLUSIONS

This study compared the seismic response of bridge piers reinforced with various rebar types of CSA 400W, CSA 500W, and ASTM A1035 Grade 690. Pushover analyses were performed to predict drifts corresponding to different damage states. It was found that bridge piers with high strength rebars have higher drift capacity corresponding to the same level of damage states, meaning that high strength rebar delays the damage. In addition, the ductility of different piers is calculated using the drifts at the Replacement Damage state and Minimal Damage State. This ratio ranges from 2.6 to 3.7, indicating the piers are generally ductile. The piers with CSA 400W, CSA 500W, and A1035 Garde 690 have average ductility of 3.2, 3.0, and 3.4. Thus, the piers with A1035 Garde 690 are the most ductile and the piers with CSA 500W are the least ductile. However, the parameters and number of analyses in this preliminary are limited and this conclusion may not be generalized. Further studies are needed to generalize this conclusion while considering higher axial load ratios, larger pier diameter, validated low cycle fatigue models for different steel reinforcements, etc.

Subsequent to the pushover analysis, nonlinear time history analyses were performed to compare the performance of bridge piers subject to earthquake ground motions. The fragility curves show that the probability of damage was generally lower for bridge piers reinforced with high strength rebars.

ACKNOWLEDGMENTS

We would like to acknowledge Nucor Steel - a North American producer for their generous donations of CSA 400W and CSA 500W reinforcing steel bars. Financial contributions of the BC Ministry of Transportation and Infrastructure and WSP Canada through the NSERC Alliance Grant were critical to conduct this research and are gratefully acknowledged.

REFERENCES

[1] Mosleh, A., Razzaghi, M. S., Jara, J., & Varum, H. (2016). Development of fragility curves for RC bridges subjected to reverse and strike-slip seismic sources.

[2] Kibboua, A., Naili, M., Benouar, D., & Kehila, F. (2011). Analytical fragility curves for typical Algerian reinforced concrete bridge piers. *Structural Engineering and Mechanics, An Int'l Journal*, *39*(3), 411-425.

[3] Karim, K. R., & Yamazaki, F. (2003). A simplified method of constructing fragility curves for highway bridges. *Earthquake engineering & structural dynamics*, *32*(10), 1603-1626.

[4] Nguyen, D. D., & Lee, T. H. (2018, April). Seismic fragility curves of bridge piers accounting for ground motions in Korea. In *IOP Conference Series: Earth and Environmental Science* (Vol. 143, No. 1, p. 012029). IOP Publishing.

[5] Avşar, Ö., Yakut, A., & Caner, A. (2011). Analytical fragility curves for ordinary highway bridges in Turkey. *Earthquake Spectra*, *27*(4), 971-996.

[6] Nielson, B. G., & DesRoches, R. (2007). Analytical seismic fragility curves for typical bridges in the central and southeastern United States. *Earthquake spectra*, *23*(3), 615-633.

[7] Billah, A. M., & Alam, M. S. (2021). Seismic fragility assessment of multi-span concrete highway bridges in British Columbia considering soil–structure interaction. Canadian Journal of Civil Engineering, 48(1), 39-51.

[8] Sarraf Shirazi, R., Pekcan, G., & Itani, A. (2018). Analytical fragility curves for a class of horizontally curved box-girder bridges. *Journal of Earthquake Engineering*, *22*(5), 881-901.

[9] Zourgui, N. H., Kibboua, A., & Taki, M. (2018). Using full bridge model to develop analytical fragility curves for typical concrete bridge piers. *bridges*, *20*, 23.

[10] Shinozuka, M., Feng, M. Q., Kim, H. K., & Kim, S. H. (2000). Nonlinear static procedure for fragility curve development. *Journal of engineering mechanics*, *126*(12), 1287-1295.

[11] SeismoSoft. 2022. SeismoStruct – a computer program for static and dynamic nonlinear analysis of framed structures. Available from https://seismosoft.com/product/seismostruct/.

[12] Montejo, L. A., and M. J. Kowalsky. 2007. CUMBIA—Set of codes for the analysis of reinforced concrete members. Technical Rep. No. IS-07-01. Raleigh, NC: North Carolina State Univ.

[13] Menegotto, M., and Pinto, P.E. 1973. Method of analysis for cyclically loaded R.C. plane frames including changes in geometry and nonelastic behavior of elements under combined normal force and bending. In Proceedings of the Symposium on the Resistance and Ultimate Deformability of Structures Acted on By Well-Defined Repeated Loads. International Association for Bridge and Structural Engineering, Zurich, Switzerland. pp.15–22.

[14] Mander, J.B., Priestley, M.J.N., and Park, R. 1988. Theoretical stress strain model for confined concrete. Journal of Structural Engineering, ASCE, 114(8): 1804–1826. doi:10.1061/(ASCE)0733-9445(1988)114:8(1804).

[15] Moyer, M. J., & Kowalsky, M. J. (2003). Influence of tension strain on buckling of reinforcement in concrete columns. *ACI Structural Journal*, *100*(1), 75-85.

[16] Restrepo, J. I., Seible, F., Stephan, B., & Schoettler, M. J. (2006). Seismic testing of bridge columns incorporating high-performance materials. *ACI Structural Journal*, *103*(4), 496.

[17] Canadian highway bridge design code. Standard CSA-S6-19. Canadian Standard Association, Rexdale, Ont.

[18] Pacific Earthquake Engineering Research (PEER). (2011). New ground motionselection procedures and selected motions for the PEER transportationresearch program. PEER Rep. 2011/03. PEER Center, University of California,Berkeley, Calif.

[19] Hancock, J., Watson-Lamprey, J., Abrahamson, N. A., Bommer, J. J., Markatis, A., McCoy, E. M. M. A., & Mendis, R. (2006). An improved method of matching response spectra of recorded earthquake ground motion using wavelets. Journal of earthquake engineering, 10(spec01), 67-89.

[20] Seismosoft. 2016. SeismoMatch – a computer program for an application capable of adjusting earthquake records, through wavelet addition. Available from https://seismosoft.com/product/seismomatch.

[21] Cornell, C. A., Jalayer, F., Hamburger, R. O., & Foutch, D. A. (2002). Probabilistic basis for 2000 SAC federal emergency management agency steel moment frame guidelines. *Journal of structural engineering*, *128*(4), 526-533.